Author(s): Puska, M. J. & Seitsonen, Ari P. & Nieminen, Risto M.

Title: Electron-positron Car-Parrinello methods: Self-consistent treatment of charge densities and ionic relaxations

Year: 1995

Version: Final published version

Please cite the original version:

Puska, M. J. & Seitsonen, Ari P. & Nieminen, Risto M. 1995. Electron-positron Car-Parrinello methods: Self-consistent treatment of charge densities and ionic relaxations. Physical Review B. Volume 52, Issue 15. 10947-10961. ISSN 1550-235X (electronic). DOI: 10.1103/physrevb.52.10947.

Electron-positron Car-Parrinello methods: Self-consistent treatment of charge densities and ionic relaxations

M. J. Puska
Laboratory of Physics, Helsinki University of Technology, FIN-02150 Espoo, Finland

Ari P. Seitsonen
Fritz-Haber-Institut der Max-Planck-Gesellschaft, Faradayweg 4-6, D-14 195 Berlin-Dahlem, Germany and Laboratory of Physics, Helsinki University of Technology, FIN-02150 Espoo, Finland

R. M. Nieminen
Laboratory of Physics, Helsinki University of Technology, FIN-02150 Espoo, Finland
(Received 22 May 1995)

A calculation method based on the two-component density-functional theory is presented for electron systems with a localized positron. Electron-ion and positron-ion interactions are described by norm-conserving pseudopotentials and full ionic potentials, respectively. The electron and positron densities are solved self-consistently using a plane-wave expansion for electron and a real-space grid method for positron wave functions, respectively. The forces on ions exerted by a positron trapped at an open-volume defect and the ensuing ionic relaxations are determined using first-principles methods. In the case of semiconductors, the self-consistent solution of electron and positron densities as well as the ionic positions are found to depend strongly on the treatment of the electron-positron correlation in constructing the effective potentials. We consider several approximations to the correlation energy while demonstrating the method by calculations for a positron trapped by a Ga vacancy in GaAs. Especially, the effects on the observable positron annihilation characteristics, i.e., positron lifetimes, core annihilation line shapes, and two-dimensional angular correlation maps are discussed.

I. INTRODUCTION

The experimental methods based on positron annihilation are powerful tools in investigating the electronic structures of solids, especially the properties of vacancy-type defects in materials.[1–3] The vacancy-type defects trap positrons due to the reduction of the repulsive nucleus-positron interaction. The trapping leads to an increase of the positron lifetime because the average electron density at a vacancy-type defect is lower than in the perfect crystal. At the same time the ratio between the annihilations with core and valence electron changes. The momentum density of the valence electrons sampled by the localized positron also deviates from its bulk value, and is reflected in the angular correlation of annihilation radiation (ACAR). As the information on electronic properties is indirect, comparisons with theoretical predictions for the positron annihilation characteristics are needed for proper interpretation of the experimental findings.[4]

The quantitative modeling of vacancy-type defects with a trapped positron is a complicated many-body problem as it involves the simultaneous determination of the electronic structure and the ionic positions around the defect. This complexity is especially true for defects in semiconductors that show (already without the trapped positron) a richness of structures and phenomena related to the coupling between the electronic states and ionic degrees of freedom.[5] On top of this, the introduction of the positron into a defect may affect considerably its electronic and ionic structure. The calculations for positron states at defects in semiconductors have thus far been mainly model calculations,[6–8] in which, e.g., the atomic positions are given as an input to the calculation, instead of full first-principles calculations without any preassumptions.

The principles for calculating positron states and annihilation characteristics have been laid down as the two-component density-functional formalism.[9] Although the formalism has been presented already several years ago, its applications have been quite scarce thus far. Recently, Gilgien *et al.*[10] demonstrated the strength of the method in the case of the singly negative As vacancy in GaAs. The calculation included also the self-consistent relaxation of the atoms around the vacancy, so that it was the first *ab initio* calculation of its kind. In semiconductors the relaxation of atoms plays a crucial role in determining the properties of defects and the importance of the positron-induced relaxation, which was earlier discussed semiempirically,[11] was treated by Gilgien *et al.* from first principles.

In the two-component density-functional theory the basic quantities are the positron and electron densities. In the case of a localized positron at a lattice defect, the positron density is finite near the defect and has an effect on the average electron density. The electron and positron densities have to be determined simultaneously, requiring the self-consistency of the solution (in the case of delocalized states the positron density is vanishingly

small everywhere, and does not affect the bulk electronic structure). The self-consistency includes the Coulombic Hartree interactions and the different exchange and correlation interactions among the charge densities. As a matter of fact, it turned out during this work that even the qualitative results can depend sensitively on the treatment of the electron-positron correlation energy. The relative importance of the electron-positron correlation energy is much larger than the electron-electron correlation energy. This is natural, because the magnitude of the former, calculated per positron in a homogeneous electron gas, is an order of magnitude larger than the electron-electron correlation energy per electron for the same electron gas density.

We have used for the electron-positron correlation energy the local-density-approximation (LDA) scheme suggested by Boroński and Nieminen[9] (BN), in which the correlation energy functional and the corresponding contributions to the effective electron and positron potentials depend on the electron and positron densities. For this scheme we introduce a two-dimensional interpolation form for the correlation energy based on Lantto's hypernetted chain approximation calculations[12] for homogeneous electron-positron plasmas with varying positron and electron densities. We have also carried out calculations using the model suggested by Gilgien *et al.*[10] (GGGC) for the electron-positron correlation energy. In this model the positron potential does not depend explicitly on the positron density, and in the case of localized positrons the effective potential is much more attractive than in the BN scheme. In model calculations, in which the ions are not allowed to relax due to positron trapping it is customary to apply the "conventional" scheme (the CONV scheme) in which the electron density is not at all affected by the positron. Then the positron potential depends only on the electron density, unperturbed by the presence of the positron. The results of this approach are in fact very similar to those obtained by the BN scheme (see below). Finally, we have made calculations also by completely omitting the electron-positron correlation in constructing the effective potentials (the NOCORR scheme). This leads to results that are in many aspects close to those obtained by the GGGC scheme.

The enhancement of the electron density at the positron, or the contact value of the electron-positron pair-correlation function, is another important electron-positron correlation quantity. It is needed in calculating the positron annihilation characteristics. In the BN scheme the enhancement depends on the electron and positron densities, and it is calculated by using an LDA interpolation form based on Lantto's hypernetted-chain-approximation calculations.[12] According to Lantto's results the contact density decreases remarkably when the positron density, at a given constant electron density, increases. In the self-consistent calculations,[9] the increase of the contact density due to the rise of the *average* electron density at a localized positron is effectively compensated by the decrease of the enhancement factor so that the positron lifetime obtained is close to that obtained by the CONV method. In the GGGC scheme the enhancement is calculated assuming that the positron density is vanishingly small. This leads to double counting in the sense that the contact density at a localized positron increases due to the increase of the average electron density and at the same time the maximum strength for the enhancement is used. This leads to overestimation in the annihilation rate when compared with the BN scheme. However, this overestimation compensates the large decrease of the annihilation rate due to the stronger positron localization in the GGGC scheme. Thus, there is a feedback effect due to the fact that the positron density relaxes following the electron density.

Due to the compensating and feedback effects the positron lifetime is not very sensitive to the model used for the electron-positron correlation if the ionic positions are kept fixed. On the contrary, the intensity of core annihilations relative to the total annihilation rate depends strongly on the degree of the localization of the positron wave function and thereby on the correlation model used. The two-dimensional ACAR (2D-ACAR) plots for the annihilations with valence electrons also reflect the localization of the positron wave function.

This work presents methods for the self-consistent calculations of the electron and positron states and the ionic structures in the case of vacancy-type defects in solids. The modern first-principles molecular-dynamics methods[13,14] applied within the frame of the two-component density-functional formalism are well suited for the actual solution of the system. Moreover, in this work we carefully discuss the above questions related to the electron-positron correlation, i.e., the buildup of the potential trapping the positron and the enhancement of the electron density at the positron determining the positron annihilation characteristics. The discussion is based on the results for a triply negative Ga vacancy in GaAs, which is an important defect studied extensively by positron annihilation measurements[15,16] and which due to its simple breathing-mode-only type relaxation pattern is well suited also for model studies. We will quantify our discussion and make comparisons with experiments by calculating the positron lifetimes, the core annihilation line shapes, and the 2D-ACAR maps with different models for electron-positron correlation.

The organization of the present paper is as follows: In Sec. II the computational methods are presented. It includes a review of the two-component density-functional theory, presentation of the new interpolation forms for the electron-positron correlation, discussion of the different schemes related to this correlation, and equations for calculating the positron annihilation characteristics. Section III contains the results and discussion for the ideal Ga vacancy in GaAs as well as for the Ga vacancy with self-consistent ionic relaxations. Section IV is a short summary.

II. COMPUTATIONAL METHODS

A. Two-component density-functional theory

Our aim is to describe from first principles the system of a positron trapped by a defect in a solid. This means that we need a calculation scheme, in which the electron

and positron densities as well as the ion positions are determined self-consistently. This can be done using the two-component density-functional theory.[9]

We write the total energy of the system as a functional of the electron density $n^e(\mathbf{r})$, positron density $n^p(\mathbf{r})$, and the ion positions $\{\mathbf{R}_I\}$:

$$E[n^e,n^p,\{\mathbf{R}_I\}]=F[n^e,\{\mathbf{R}_I\}]+F[n^p,\{\mathbf{R}_I\}] +E_H[n^e,n^p]+E_c^{e\text{-}p}[n^e,n^p] +E_{\text{ion}}(\{\mathbf{R}_I\}) . \quad (1)$$

Above, $E_H^{e\text{-}p}[n^e,n^p]$ is the Coulomb (Hartree) interaction between the electron and positron densities and $E_c^{e\text{-}p}[n^e,n^p]$ is the correlation energy between electrons and positrons. $F[n,\{\mathbf{R}_I\}]$ are the one-component functionals for either the electron or the positron density, i.e.,

$$F[n\{\mathbf{R}_I\}]=E_{\text{kin}}[n]+E_{\text{ext}}[n,\{\mathbf{R}_I\}] +E_H[n]+E_{\text{xc}}[n] , \quad (2)$$

where $E_{\text{kin}}[n]$, $E_H[n]$, and $E_{\text{xc}}[n]$ are the usual kinetic energy, Hartree energy, and exchange-correlation energy functionals of the one-component density-functional theory, respectively. $E_{\text{ext}}[n,\{\mathbf{R}_I\}]$ is the interaction energy between the charge density n and the nuclei Z_I at the positions $\{\mathbf{R}_I\}$. The ground state of the system is found by minimizing the total-energy functional $E[n^e,n^p,\{\mathbf{R}_I\}]$. We do this by using for the total-energy functional a generalized Kohn-Sham form, in which the electron density is obtained from the auxiliary one-particle wave functions $\psi_i^e(\mathbf{r})$:

$$n^e(\mathbf{r})=\sum_i^{\text{occ}}|\psi_i^e(\mathbf{r})|^2 . \quad (3)$$

Above, the summation is over all occupied electron states. Because in the relevant experiments there is only one positron in the sample at a given time, the positron density corresponds to a single wave function

$$n^p(\mathbf{r})=|\psi^r(\mathbf{r})|^2 . \quad (4)$$

In practice, only the valence part n^v of the electron density is calculated self-consistently. For the core electron density n^c the free-atom distribution is used; i.e., it is assumed not to be affected by the solid environment or by the presence of the positron. The interactions between the valence electrons and the ion cores are described within the pseudopotential model. The electron wave functions are presented by plane-wave expansions, the coefficients of which have to be determined. This means that the part $F[n^e,\{\mathbf{R}_I\}]+E_{\text{ion}}(\{\mathbf{R}_I\})$ of the total-energy functional is treated within the usual pseudopotential formalism explained, for example, in Refs. 14 and 17. For the positron-ion core interactions core densities of free atoms are used. The positron wave function is solved in real space using a method[18] based on the conjugate gradient optimization.[14] The real-space point grid is the same as used in performing the fast Fourier transformations in the plane-wave approach for the valence electrons and this grid couples the valence electron and positron densities.

Our calculation for a positron trapped by a defect proceeds as follows. First the positions of the ions are kept fixed and the corresponding electron density is calculated without the effect of the positron. The Fourier coefficients of the valence electron wave functions are determined by a steepest-descent minimization of the pure electronic part $F[n^e,\{\mathbf{R}_I\}]$ of the total-energy functional. Then the electron density is kept fixed and the positron wave function is calculated in the points of the real-space grid by minimizing the terms containing the positron density, i.e., $F[n^p,\{\mathbf{R}_I\}]+E_H[n^e,n^p]+E_c^{e\text{-}p}[n^e,n^p]$. Thereafter the electron density is iterated by including also the cross terms containing the positron density. The whole electron-positron system is then iterated to self-consistency by repeating a sequence in which the positron density is updated always after every electronic iteration. When the self-consistency of the electron and positron densities is achieved, the forces acting on the different ions I are calculated using the Hellman-Feynman theorem as

$$\mathbf{F}_I=-\frac{\partial E[n^e,n^p,\{\mathbf{R}_I\}]}{\partial \mathbf{R}_I} . \quad (5)$$

The ions are moved according to these forces using a damped second-order dynamics algorithm. The electron density and the positron density following it are relaxed simultaneously with the relaxation of the ions using fictitious dynamics for the coefficients of the electron wave functions.

In the LDA of the density-functional theory for electronic structure a localized electron interacts with itself, because the Hartree and exchange-correlation terms in the energy functional Eq. (2) are calculated using the total density. The situation is in a way most pathological for a one-electron system, such as the hydrogen atom. The self-interaction in this case means that the attractive $-1/r$ Coulomb potential due to the nucleus is substituted at large distances by the short-range exchange-correlation potential. In the self-interaction correction method (Ref. 19) the Hartree and exchange-correlation energies of a given localized electron with itself are assumed to cancel each other. Then, for example, the potential in the hydrogen atom is corrected to the attractive long-range $-1/r$ Coulomb potential. Because there is only one localized positron in the systems considered in this work, we explicitly make, following Boroński and Nieminen,[9] the self-interaction correction for the positron. The functional F for the positron density simplifies then as

$$F[n^p,\{\mathbf{R}_I\}]=E_{\text{kin}}[n^p]+E_{\text{ext}}[n^p,\{\mathbf{R}_I\}] . \quad (6)$$

In the case of a positron trapped at a defect the SIC means that the positron potential far from the defect is a long-range Coulomb potential due to the extra electron charge relaxed towards the center of the defect to screen the positron. This long-range potential results in a more localized positron wave function than the short-range LDA potential.

The terms of the total-energy functional

$E[n^e, n^p, \{\mathbf{R}_I\}]$ that do not contain the positron density are treated within the usual pseudopotential formalism. The positron kinetic energy is calculated in the real-space grid using a five-point difference formula. The evaluation of the electrostatic terms containing the positron density is briefly commented on below and the crucial treatment of the electron-positron correlations is explained more carefully in Sec. II B.

The electrostatic terms containing the positron density in Eq. (1) are

$$E_{\text{ext}}[n^p,\{\mathbf{R}_I\}]+E_H[n^e,n^p]=\sum_I \int \frac{Z_I n^p(\mathbf{r})}{|\mathbf{r}-\mathbf{R}_I|}d\mathbf{r}-\int\int \frac{n^p(\mathbf{r})[n^v(\mathbf{r}')+n^c(\mathbf{r}')]}{|\mathbf{r}-\mathbf{r}'|}d\mathbf{r}'\,d\mathbf{r}\ , \tag{7}$$

where the electron density has been divided into valence n^v and core n^c parts. The integral involving the core electron charge and the corresponding part of the nucleus-positron interaction are performed in real space. The valence-electron-positron interaction is performed as a sum in the reciprocal lattice by first Fourier transforming the positron density calculated in real space. Actually, the Fourier-transformed Hartree potential due to the valence electron density and positive Gaussian charge distributions describing the valence part of the nucleus is first calculated. Then, in the summation over the reciprocal lattice vectors the $\mathbf{G}=0$ term is excluded. This exclusion is done also in calculating the valence electron-ion interaction. Thus, in the case of a supercell with a nominal net charge there will be an implicit neutralizing background charge and there are no long-range Coulomb interactions between the cells of the superlattice. Finally, the use of the Gaussian distribution instead of a pointlike one is corrected by a summation in real space, in a fashion similar to the ordinary Ewald summation.

The effective potentials needed in the electron and positron Hamiltonians are obtained from the total energy as functional derivatives with respect to the electron or positron densities. The effective potential for the electrons reads

$$V_e(\mathbf{r})=\frac{\delta E_{\text{tot}}}{\delta n^e(\mathbf{r})}=V_{\text{ff}}^v(\mathbf{r})-\int\frac{n^p(\mathbf{r}')}{|\mathbf{r}-\mathbf{r}'|}d\mathbf{r}'+\frac{\delta}{\delta n^e}E_c^{e\text{-}p}[n^e(\mathbf{r}),n^p(\mathbf{r})]\ , \tag{8}$$

where V_{eff}^v is the usual one-component effective electron potential (containing in our scheme, e.g., the local and nonlocal pseudopotential terms). Similarly, the effective positron potential is

$$V_p(\mathbf{r})=\frac{\delta E_{\text{tot}}}{\delta n^p(\mathbf{r})}=\sum_I\frac{Z_I}{|\mathbf{r}-\mathbf{R}_I|}-\int\frac{n^e(\mathbf{r}')}{|\mathbf{r}-\mathbf{r}'|}d\mathbf{r}'+\frac{\delta}{\delta n^p}E_c^{e\text{-}p}[n^e(\mathbf{r}),n^p(\mathbf{r})]\ . \tag{9}$$

These equations define the electron-positron correlation potentials for electron $((\delta/\delta n^e)E_c^{e\text{-}p}[n^e(\mathbf{r}),n^p(\mathbf{r})])$ and positron $((\delta/\delta n^p)E_c^{e\text{-}p}[n^e(\mathbf{r}),n^p(\mathbf{r})])$ states.

B. Electron-positron correlation energy

When a positron enters the electron system of a solid, it gathers a screening cloud of electrons around it. In the two-component formalism for a positron trapped by a defect the screening cloud consists of the relaxation of the "average" electron density n^e towards the localized positron density n^p and of the "short-range" correlation cloud when the positron is thought to be fixed in a given point in the system. In the total-energy functional the first effect of screening enters through the electron-positron Hartree interaction term in Eq. (1). The correlation part is included in the (unknown) functional $E_c^{e\text{-}p}[n^e,n^p]$. Besides the correlation energy functional the correlation effects manifest themselves through the positron-electron contact density (the so-called enhancement factor) used in calculating the annihilation rate. We will first consider the approximation for the correlation energy.

Boroński and Nieminen[9] introduced the LDA for the electron-positron correlation energy in the two-component theory by a function $F_c^{e\text{-}p}$ defining the correlation energy per *unit volume* at a given point. (In the one-component LDA one defines the exchange-correlation energy per particle.) The arguments of $F_c^{e\text{-}p}$ are the local electron and positron densities and the total electron-positron correlation energy of the system is obtained by integrating over the volume

$$E_c^{e\text{-}p}(n^e,n^p]=\int F_c^{e\text{-}p}(n^e(\mathbf{r}),n^p(\mathbf{r}))d\mathbf{r}\ . \tag{10}$$

The electron and positron correlation potentials, which are defined as the functional derivatives of the correlation energy with respect to the electron or positron density [see Eqs. (8) and (9)], are then simple partial derivatives of the function $F_c^{e\text{-}p}(n^e,n^p)$:

$$V_e^{e\text{-}p}(\mathbf{r})=\frac{\partial F_c^{e\text{-}p}(n^e(\mathbf{r}),n^p(\mathbf{r}))}{\partial n^e}\ ,\qquad V_p^{e\text{-}p}(\mathbf{r})=\frac{\partial F_c^{e\text{-}p}(n^e(\mathbf{r}),n^p(\mathbf{r}))}{\partial n^p}\ . \tag{11}$$

One reason for the few applications of the two-component density-functional formalism has been the lack of accurate interpolation forms for the electron-positron correlation energy in the LDA. The interpolation form presented by Boroński and Nieminen[9] was

based on symmetry arguments and on Lantto's[12] hypernetted chain calculations for systems of equal electron and positron densities, and on a different type of many-body calculations by Arponen and Pajanne[20] for the limit of a delocalized positron in a homogeneous electron gas. The scarcity of the data leads to difficulties in the construction of the interpolation form for correlation energy for the whole electron-positron density plane. The clearest manifestation of the difficulties is the nonmonotonic behavior of the correlation potentials derived from the interpolation form of Boroński and Nieminen.

Lantto[12] has later published more data for the electron-positron correlation energy, including several ratios of the electron and positron densities. On the basis of the these data we have constructed a new well-behaving interpolation form $F_c^{e\text{-}p}(n^e,n^p)$. The ratio of the electron and positron densities is denoted as

$$x = n^p/n^e \ . \tag{12}$$

Lantto has given the correlation energy for eight x values in the range $x=0,\ldots,1$ for electron densities with $r_s^e=1$, 2, 3, 4, and 5 a.u. We require that the function $F_c^{e\text{-}p}(n^e,n^p)$ is symmetric with respect to the change of the positron and electron densities. Furthermore, we require that in the limit of vanishing positron density the form

$$E_c^{e\text{-}p}[n^e,n^p]=E_c^{e\text{-}p}[n^e,n^p\to 0] = \int n^p(\mathbf{r})\epsilon_{\mathrm{AP}}(n^e(\mathbf{r}))d\mathbf{r} \ , \tag{13}$$

is obtained. Above, $\epsilon_{\mathrm{AP}}(n)$ is the correlation energy for a delocalized positron in a homogeneous electron gas. Due to symmetry, a corresponding form is required on the limit of vanishing electron density. We have used for $\epsilon_{\mathrm{AP}}(n)$ the results calculated by Arponen and Pajanne[20] as parametrized by Boroński and Nieminen.[9]

For the interpolation we use the functional form

$$\frac{1}{E_c^{e\text{-}p}(n^e,n^p)} = a(r_s^e)+b(r_s^e)r_s^p+c(r_s^e)(r_s^p)^2 + \frac{4\pi}{3}\frac{(r_s^p)^3}{\epsilon_{\mathrm{AP}}(r_s^e)}+\frac{4\pi}{3}\frac{(r_s^e)^3}{\epsilon_{\mathrm{AP}}(r_s^p)} \ . \tag{14}$$

where $r_s^e(r_s^p)$ is the electron (positron) density parameter defined by $n^e=3/[4\pi(r_s^e)^3]$ ($n^p=3/[4\pi(r_s^p)^3]$). The symmetry with respect to r_s^p and r_s^e means that the functions $a(r_s^e)$, $b(r_s^e)$, and $c(r_s^e)$ are second-order polynomials,

$$\begin{aligned} a(r_s^e) &= A_a+B_a r_s^e+C_a(r_s^e)^2 \ , \\ b(r_s^e &= B_a+B_b r_s^e+C_b(r_s^e)^2 \ , \\ c(r_s^e) &= C_a+C_b r_s^e+C_c(r_s^e)^2 \ . \end{aligned} \tag{15}$$

The coefficients are determined by the linear least-squares fit to Lantto's data.[12] When the densities and the r_s parameters are given in a.u. and the correlation energy in Ry the coefficients have the values

$$\begin{aligned} &A_a=69.7029, \quad B_a=-107.4927, \quad C_a=23.7182 \ , \\ &B_v=141.8458, \quad C_b=-33.6472, \quad C_c=5.21152 \ . \end{aligned} \tag{16}$$

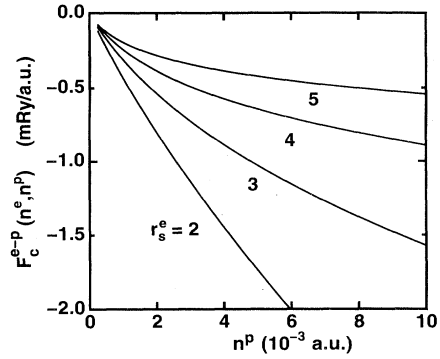

FIG. 1. Electron-positron correlation energy per unit volume $F_c^{e\text{-}p}(n^e,n^p)$. The energy is shown as a function of the positron density for various values of the electron density. The figure is based on the interpolation form of Eq. (14).

The above fit behaves well around the typical electron and positron densities at vacancies in semiconductors ($r_s^e \simeq r_s^p \simeq 3$ a.u.). The fit is, however, based on results with $r_s \geq 1$ a.u., only. In the ion-core region where r_s^e is less than unity and r_s^p is very large, one should in practical calculations of the correlation energy smoothly switch to the form of Eq. (13) for the vanishing positron density. We use the matching point of $r_s^e=0.7$ a.u. The small errors introduced to the positron correlation energy in this substitution are not important, because in the high-density ion core region the positron wave function is very small. The errors in the positron correlation potential are not important, because the Coulomb repulsion dominates over the correlation.

The resulting electron-positron correlation energy densities are shown in Fig. 1 as a function of the positron density. Although the qualitative behavior of the curves in Fig. 1 is the same as that in the corresponding figure given by Boroński and Nieminen[9] there are important

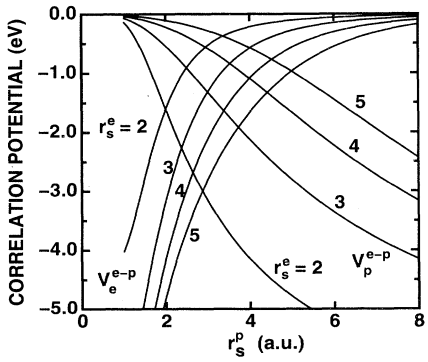

FIG. 2. Electron-positron correlation potentials for electrons $V_e^{e\text{-}p}(n^e,n^p)$ and positrons $V_p^{e\text{-}p}(n^e,n^p)$. The potentials are shown as a function of the positron density parameter for various values of the electron density. The figure is based on the interpolation form of Eq. (14).

quantitative differences between the two results. The main reason for the differences can be traced back to the scarcity of the original data used in Ref. 9. The electron and positron parts of the electron-positron correlation potential calculated according to Eq. (11) from the correlation energy are shown in Fig. 2. For a fixed electron density, the positron part rises rapidly as the positron density increases (to the left in the figure). This means that the number of electrons becomes more and more insufficient to screen the positron density. The present potentials are more repulsive than those given in Ref. 9 and, for example, the positron potentials decay towards the results of the vanishing positron limit more slowly than in the old interpolation results.

C. Different schemes for calculating localized positron states

The use of the electron-positron correlation energy in the LDA [Eq. (10)] and the corresponding determination of the annihilation characteristics (Sec. II D below) constitutes the two-component BN calculation scheme. As mentioned in the Introduction, for the description of the localized positron states there exists also the CONV scheme relying on the normal one-component density-functional theory. Moreover, the GGGC scheme represents a different type of two-component approach. In this subsection we describe the calculation of the electron and positron states in these schemes. The description of the calculation of the annihilation characteristics is postponed to Sec. II D.

In the case of a delocalized positron in a perfect crystal lattice the positron density is vanishingly small at every point. Therefore the electron density is not affected by the positron and can be calculated as in the usual one-component formalism. From the electron density, the positron potential is constructed in the limit of the vanishing positron density in accordance with Eqs. (9) and (13) as

$$V^p(\mathbf{r})=V_{\mathrm{Coul}}(\mathbf{r})+\epsilon_{\mathrm{AP}}(n^e(\mathbf{r}))\ , \tag{17}$$

where the Coulomb part V_{Coul} arises from the nuclei and the electron density. Then the positron wave function is solved. No self-consistency iterations are needed when introducing the positron.

The procedure for delocalized positron states is remarkably simpler than the full two-component scheme required for the localized positron states. For this reason and also because of the lack of the two-component electron-positron correlation functional the procedure has been widely used also for localized positron states. This procedure is the above-mentioned CONV scheme. It can be justified by arguing that the positron together with its screening cloud enters the system as a neutral quasiparticle, which does not affect the average electron density. The two-component and the CONV schemes can be (to some extent) viewed as two different ways to divide the total positron potential in to the correlation part and the Coulomb part: In the CONV scheme the effects of the positron screening are taken into account only via the electron-positron correlation potential whereas in the two-component theory they contribute, due to the relaxation of the electron density, also via the Hartree term. In the two-component theory the correlation part decreases in magnitude when the positron density increases and this opposes the lowering of the Hartree part due to the increase of the electron density relative to the CONV scheme (near the regions where the positron density is high). As a result, as will be seen below, the positron density and the ensuing positron annihilation characteristics calculated with the CONV and the BN-LDA scheme are very similar (if the ion positions are kept fixed). The differences in the annihilation characteristics are damped also because the increase of the annihilation rate due to the increase of the average valence electron density near the localized positron is compensated due to the decrease of the (correlation) contact density as the positron density increases.

In the two-component GGGC scheme the positron potential does not depend on the positron density. This is achieved by using in the LDA a two-component electron-positron correlation energy in the limit of vanishing positron density [Eq. (13)] irrespective of the actual value of the positron density. The model makes the implementation of the two-component scheme easy, because for a given electron density the positron state can be directly calculated without (positron) self-consistency iterations that are necessary in the BN scheme. The model can be justified[10] also by the fact that it is free from positron self-interaction in the sense that the positron potential does not depend on the positron density at all (in the BN scheme the positron potential depends on the positron potential via the electron-positron correlation potential). However, the GGGC scheme clearly overestimates the electron-positron correlation effects: The positron potential is lowered via the Coulomb (Hartree) term and at the same time the positron correlation potential is calculated so that it has the maximum strength, which appears for the vanishing positron density. According to Fig. 3, for the electron and positron density parameters $r_s^p=r_s^e=3$ a.u. corresponding to

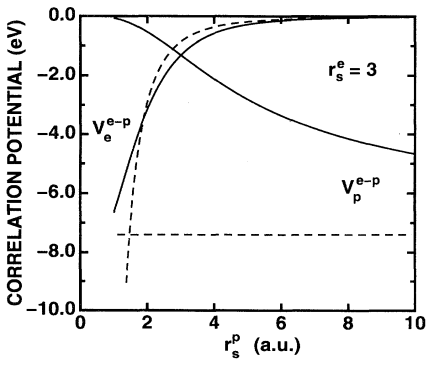

FIG. 3. Electron-positron correlation potentials for electrons $V_e^{e\text{-}p}(n^e,n^p)$ and positrons $V_p^{e\text{-}p}(n^e,n^p)$. The potentials are shown as a function of the positron density parameter for the electron density parameter $r_s^e=3$ a.u. The solid lines are based on the interpolation form of Eq. (14) whereas the dashed lines correspond to the limit of vanishing positron density, Eq. (13).

roughly the situation in a semiconductor vacancy, the positron correlation potential is almost 6 eV lower in the GGGC scheme than in the BN scheme with the new interpolation function. This leads to very localized positron states at defects. Gilgien *et al.*[10] report even self-trapping of the positron in the interstitial region of the *perfect* GaAs lattice. Mobility measurements[21] by the slow-positron-beam technique clearly rule out positron self-trapping.

D. Positron annihilation characteristics

In the two-component LDA calculations the positron annihilation rate as a function of the momentum $\mathbf{p}$ of the annihilating positron electron pair is determined as

$$\rho(\mathbf{p})=\pi r_e^2 c \sum_i \left| \int e^{i\mathbf{p}\cdot\mathbf{r}} \psi^p(\mathbf{r})\psi^e(\mathbf{r}) \times \sqrt{g(n^e(\mathbf{r}),n^p(\mathbf{r}))}\, d\mathbf{r} \right|^2 , \quad (18)$$

where r_e is the classical electron radius and c is the speed of light. The summation is over all occupied electron states. For the enhancement factor (the contact density) $g(n^e,n^p)$ we use the functional form introduced by Boroński and Nieminen[9] for interpolating in the plane of electron and positron densities. The form includes the function g_0 for the limit $n^p \to 0$, g_1 for the case of $n^p=n^e$, and g_2 for the case of $n^p=n^e/2$. We have obtained the coefficients of these functions by fitting Lantto's data quoted by Boroński and Nieminen.[9] The resulting functions are (r_s in a.u.)

$$g_0(r_s)=1+1.23r_s+0.98890r_s^{3/2} -1.4820r_s^2+0.3956r_s^{5/2}+r_s^3/6 , \quad (19)$$

$$g_1(r_s)=1+2.0286r_s-3.3892r_s^{3/2} +3.0547r_s^2-1.0540r_s^{5/2}+r_s^3/6 , \quad (20)$$

$$g_2(r_s)=1+0.2499r_s+0.2949r_s^{3/2} +0.6944r_s^2-0.5339r_s^{5/2}+r_s^3/6 . \quad (21)$$

These interpolation forms differ slightly from the fits made by Boroński and Nieminen.[9]

The total annihilation rate is obtained from Eq. (18) by integrating over the momentum. The result is

$$\lambda=\pi r_e^2 c \int n^p(\mathbf{r})n^e(\mathbf{r})g(n^e(\mathbf{r}),n^p(\mathbf{r}))d\mathbf{r} . \quad (22)$$

In the LDA for positron annihilation the total annihilation rate is divided into core (λ_c) and valence (λ_v) contributions as[22]

$$\lambda_c = \int n^p(\mathbf{r})g(n^e(\mathbf{r}),n^p(\mathbf{r}))n^c(\mathbf{r})d\mathbf{r} , \quad (23)$$

$$\lambda_v = \int n^p(\mathbf{r})g(n^e(\mathbf{r}),n^p(\mathbf{r}))n^v(\mathbf{r})d\mathbf{r} .$$

In the CONV scheme for localized positrons at defects in solids the annihilation rate is calculated on the limit of the vanishing positron density, i.e., also the contact electron density is treated as for delocalized positrons and the enhancement function $g_0(r_s)$ is used. The CONV scheme has been in wide use and it gives positron lifetimes at vacancies that are in a reasonable agreement with the experimental results for metals and also for semiconductors, if reasonable ionic relaxations around the vacancy are assumed.[7,8]

In the two-component GGGC scheme the enhancement function $g_0(r_s)$ on the limit of the vanishing positron density is used. Because this enhancement factor is larger than the two-component value with the same electron density but with a finite positron density, the approximation shortens the positron lifetime. This acts to cancel the tendency of the model to increase the positron lifetime via the strong positron localization.

The magnitude of the core annihilation rate is monitored by the so-called core annihilation or W parameter of the line-shape measurements.[3] It is defined as the ratio of the annihilations occurring inside a given high-momentum window to the total number of annihilations. Because at high enough momenta only the annihilations with core electrons contribute, the changes in the W parameter reflect changes in the relative intensity of the core annihilation and thereby changes in the positron-core-electron overlap. Usually one calculates the ratio between the W parameter for a sample containing a certain defect type and the W parameter corresponding to the perfect crystal lattice. This ratio is called the relative W parameter. The relative W parameter can be estimated from the theoretical core annihilation momentum distributions.[3] However, an approximation based on the total core annihilation rates already gives a good account for its magnitude. When integrated over momentum, the shape parameter W can be written as

$$W=\frac{(\lambda_c/\lambda)^{\text{Defect}}}{(\lambda_c/\lambda)^{\text{Free}}} , \quad (24)$$

where λ_c and λ are the annihilation rate with core electrons and the total annihilation rate, respectively, calculated for a positron trapped at the defect or for a free positron. In this work we use the LDA model of Eqs. (22) and (23) for λ and λ_c, respectively.

The positron trapping rate, at which the transition form the delocalized positron state to the localized one takes place, is an important experimental parameter. Its temperature dependence gives information about the charge state of the defect.[23] Its magnitude gives an estimate for the defect concentration, provided that the trapping coefficient, i.e., the trapping rate per unit defect concentration is known. Theoretically, the type of trapping process, with a certain mechanism of the energy transfer to the host, depends crucially on the amount of energy released by the positron in the transition from the delocalized to the localized state. This is true also for the magnitude of the trapping rate. The energy release in the process is called the trapping energy. In the CONV scheme the trapping energy is calculated as the difference

of the positron energy eigenvalues for the bulk and vacancy systems. In the two-component formalism one has to consider the whole total-energy functional. The trapping energy is then

$$E_t = E_{\text{tot}}(\text{bulk}+e^+) - E_{\text{tot}}(\text{bulk}) - [E_{\text{tot}}(\text{defect}+e^+) - E_{\text{tot}}(\text{defect})] , \quad (25)$$

where the terms on the right-hand side refer to the total energy of the perfect bulk lattice with a positron, that without a positron, the total energy of the defect with a positron, and that of a defect lattice, respectively. The energy difference $E_{\text{tot}}(\text{bulk}+e^+) - E_{\text{tot}}(\text{bulk})$ is equal to the positron energy eigenvalue in the bulk for the CONV scheme as well as for the GGGC scheme.

III. RESULTS AND DISCUSSION

We demonstrate the calculation scheme in the case of the III-V compound semiconductor GaAs, considering the Ga vacancy in the triply negative charge state. The electron-ion interactions are described by norm-conserving pseudopotentials.[24] The omittance of Ga, *d*-states and the overlap of core and valence electron densities are (partially) corrected using the nonlinear core-valence exchange-correlation scheme.[25] Besides the local part (*d* component) the pseudopotentials contain nonlocal *s* and *p* components. In the plane-wave expansions for the electron states we use the cutoff energy of 16.8 Ry, which corresponds to about 11 000 plane waves per eigenstate. We use a cubic supercell with periodic boundary conditions. The supercell contains 64 (63) atoms in the case of the perfect bulk lattice (the Ga vacancy). Only the Γ point is used to sample the first Brillouin zone. In calculating the relaxations of the ions around the vacancy with molecular dynamics we use the true physical masses of the ions and the fictitious mass of 400 a.u. for the electronic states. The time step of 6 a.u. is used in solving the equations of motion.

Our calculations for the perfect bulk lattice gives the lattice constant of 5.62 Å, which is in good agreement with the experimental value of 5.65 Å.[26] The positron bulk lifetime calculated in the CONV scheme is 214 ps. By construction, this is the bulk lifetime for the BN and GGGC two-component schemes also. The positron bulk lifetime calculated without the electron-positron correlation potential (in the NOCORR scheme) is, due to the reduced annihilation near the ion ones, a somewhat longer 227 ps. The calculated positron lifetimes are shorter than the experimental value of 231 ps (Ref. 15). This is partly due to the smaller lattice constant, but the main reason is that the LDA in calculating the positron annihilation rate leads to generally too short positron lifetimes.[27] The error is, for a wide range of materials and positron lifetimes, proportional to the positron lifetime itself.[28] Therefore a simple scaling [in the case of the interpolation form by Boroński and Nieminen[9] the scaling factor is ~ 1.1 (Ref. 28)] can be used to correct the LDA lifetimes to agree well with experiments. In this work, we will therefore scale positron lifetimes for vacancies by the factor of $231/214 \approx 1.08$ with the exception of the values obtained without the correlation potential for which the scaling factor is $231/227 \approx 1.02$.

A. Ideal Ga vacancy in GaAs

First we want to compare the results of the different schemes for calculating the positron annihilation characteristic for a defect trapping a positron. In order to simplify the comparison we have solved for the self-consistent electron structure and the positron state for an *ideal* triply negative Ga vacancy (V_{Ga}^{3-}) in GaAs. The ionization levels of the Ga vacancy lie in the lower half of the band gap, and therefore the triply negative charge state corresponds to the experimental situation in semi-insulating and *n*-type GaAs. The ideal vacancy means that the ions are not allowed to relax from their ideal lattice positions.

The electron and positron densities obtained in the different schemes are compared in Fig. 4, which shows them on the line going through the center of the vacancy along the [111] direction. A similar comparison for the total positron potential and its Hartree and correlation components is given in Fig. 5. Figures 4(a) and 5(a) correspond to the CONV scheme, in which the electron density is calculated without the influence of the positron and the positron state is determined without self-consistency iterations. In Figs. 4(b) and 5(b) the results obtained in the two-component BN scheme and in Figs. 4(c) and 5(c) those of the GGGC scheme are shown. Finally, Figs. 4(d) and 5(d) show the densities and potentials for the NOCORR scheme. Comparing the two upper-

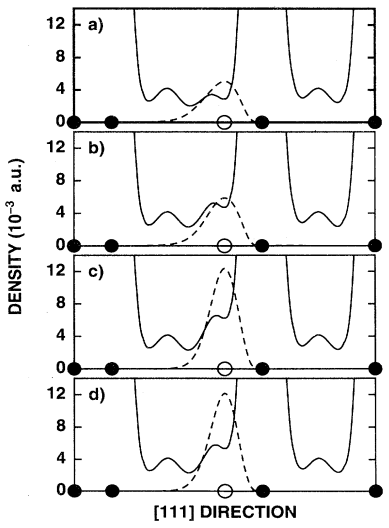

FIG. 4. Electron and positron densities in the ideal triply negative Ga vacancy in GaAs. The results are shown for the CONV scheme (a), and for the two-component BN (b), GGGC (c), and NOCORR schemes (d). The electron (positron) density is given by a solid (dashed) curve along the line in the [111] direction through the center of the vacancy (open circle) and Ga and As atoms (filled circles).

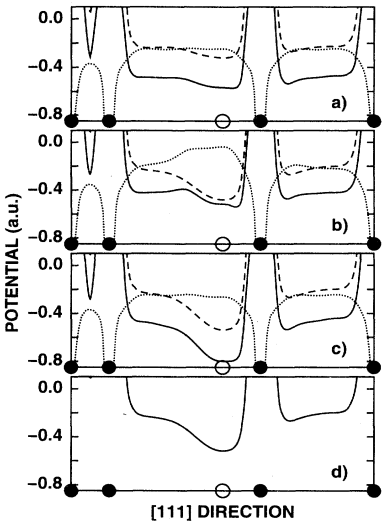

FIG. 5. Positron potential in the ideal triply negative Ga vacancy in GaAs. The results are shown for the CONV scheme (a), and for the two-component BN (b), GGGC (c), and NOCORR schemes (d). The total potential (solid curve) with its decomposition into the Hartree (dashed curve) and the correlation (dotted curve) are shown along the line in the [111] direction through the center of the vacancy (open circle) and Ga and As atoms (filled circles).

most panels of Fig. 4 it can be seen that the average electron density at the vacancy clearly increases from Fig. 4(a) to Fig. 4(b), but the positron densities are closer to each other. In the GGGC scheme the increase of the electron density is according to Fig. 4(c) somewhat stronger than in the BN scheme, but the maximum positron density is by a factor of two larger than in the CONV or in the BN scheme. The positron density obtained in the NOCORR scheme is according to Fig. 4(d) nearly the same as in the GGGC scheme. The electron density at the vacancy is slightly lower in Fig. 4(d) than in Fig. 4(c) due to the omission of the attractive electron part of the electron-positron correlation.

Figure 5, which shows the positron potentials, explains nicely the trends seen in the positron density. In the two-component BN scheme the total positron potential is quite similar to that in the CONV scheme. This is a result of the cancellation of the changes in the Hartree potential and in the correlation potential when the model for the positron screening changes from the conventional one to that of the two-component theory. It can be seen that the Hartree potential is lowered when the electron density at the vacancy increases, but the two-component correlation potential rises when the positron density increases. In the GGGC scheme this cancellation does not occur, because, to a rather good approximation, the correlation potential is the same as in the CONV scheme whereas the Hartree potential is close to that obtained also in the BN scheme.

In the two-component NOCORR calculation the total potential of the positron consists only of the Hartree term, which to a high accuracy is the same as that obtained in the GGGC scheme. Because the correlation potential in the GGGC scheme is quite structureless inside the vacancy, its omission does not affect the positron density. In the CONV scheme the omission of the positron correlation potential improves the positron localization at the vacancy, because due to the higher electron density the correlation potential is more attractive in the interstitial regions than at the vacancy. When the electron density is then allowed to relax in a two-component calculation the localization is further improved due to the accumulation of the screening electron charge at the vacancy.

Figure 6 shows the contour map of the relaxation of the electron density due to the introduction of the positron into the ideal Ga vacancy. This map is obtained as a difference between the electron density calculated with the positron using the BN scheme and that of a clean vacancy. The electron density decreases quite evenly from the bond regions far from the vacancy. Close to the vacancy the screening charge shows maxima at the dangling bonds. Thus, the positron shows a tendency towards to healing the effects of the vacancy to the bulk electronic structure.

The positron lifetimes, core and valence annihilation rates, as well as the trapping energies at the ideal triply negative Ga vacancy calculated in different schemes are shown in Table I. The lifetimes and partial annihilation rates are scaled so that the bulk lifetime coincides with the experimental one of 231 ps (see the discussion above). The CONV scheme calculation as well as the two-component BN and GGGC schemes give quite similar lifetimes, 270–278 ps. Also the calculation with the NOCORR scheme gives a similar result, 264 ps, if the enhancement is taken in the limit of the vanishing positron density. The fact that the CONV scheme and the GGGC scheme give practically the same positron lifetime is a result of a feedback effect:[29] Both schemes use the same functions for the construction of the positron potential and the annihilation rate. Then, if the electron

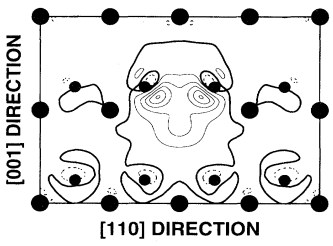

FIG. 6. Electron density induced by a positron trapped by the ideal triply negative Ga vacancy in GaAs. The two-component scheme by Boroński and Nieminen is used. The figure shows a region of the (110) plane limited by the borders of the simulation cell. The contours of the positive (negative) values are shown as solid (dashed) curves. The contour of the zero density is denoted by a bold solid line. The contour spacing is one-sixth of the maximum value.

TABLE I. Positron lifetime τ, core annihilation rate λ_c, valence annihilation rate λ_v, relative W parameter [Eq. (24)], and trapping energy E_t at the ideal triply negative Ga vacancy in GaAs. The results of the CONV scheme, the two-component calculations within BN, GGGC, and NOCORR schemes are given. The lifetimes and annihilation rates are scaled so that the theoretical bulk lifetime coincides with the experimental one of 231 ps (Ref. 15). In the two last cases the lifetimes given in the parentheses are obtained using the two-component form of Eq. (22) depending on both the electron and positron densities. The annihilation rates for the perfect bulk lattice calculated using the correlation potential (CONV) or without using it (NOCORR) are given for comparison.

Scheme	τ (ps)	λ_c (1/ns)	λ_v (1/ns)	W	E_t (eV)
Ideal vacancy					
CONV	270	0.279	3.422	0.59	0.73
BN	278	0.292	3.304	0.65	0.60
GGGC	270 (311)	0.154	3.546	0.32	2.46
NOCORR	264 (308)	0.135	3.649	0.33	2.64
Bulk					
CONV	231	0.554	3.775		
NOCORR	231	0.468	3.861		

density changes, due to approximations used in its construction or in the present two-component formalism due to the finite positron density, the positron density follows the electron density in such a way that the electron-positron overlap and the annihilation rate are conserved. In the present case the strength of the feedback effect is obvious because the changes in the electron and especially in the positron densities between the CONV and the GGGC methods are very large (see Fig. 4). The similarity of the lifetimes of the CONV and the BN schemes is a result of the near cancellation of the increase of the annihilation rate due to the increased electron density and the decrease the annihilation rate due to the finite positron density when switching from the former scheme to the latter.[9]

According to Table I, the annihilation rate for the core electrons is much more sensitive to the calculation scheme than the positron lifetime. The CONV and the BN schemes give for the ideal Ga-vacancy practically the same core annihilation rate of ~ 0.3 ns^{-1}. The GGGC and NOCORR schemes gives core annihilation rates smaller by approximately a factor of two. The reduction seen in the GGGC and NOCORR schemes relative to the CONV and the BN schemes is due to the stronger positron localization in the former. The relative W parameters, calculated from Eq. (24) using the annihilation rates of the CONV and BN schemes give similar results, i.e., 0.59 and 0.65, respectively. The values from the GGGC and NOCORR are remarkably lower, 0.32 and 0.33, respectively. The relative W parameter measured for the Ga vacancy by the standard Doppler broadening technique is 0.89 (Ref. 30), while high-resolution coincidence-Doppler measurements give values between 0.7 and 0.8 (Ref. 31). Thus, these experiments strongly support the CONV and the BN schemes in the comparison with the GGGC and NOCORR schemes. This conclusion is even strengthened when the relaxation of the ions around the vacancy is considered below.

We have also calculated the positron lifetimes by using the electron and positron densities of the GGGC scheme but employing the two-component enhancement factor. This kind of calculation is also done with densities obtained with the NOCORR scheme. The resulting lifetimes, which are shown in parentheses in Table I, are remarkably long. This is a result of the strong positron localization at the open volume of the vacancy. The increase of the positron lifetime is opposed in the GGGC and NOCORR schemes when the enhancement at the limit of the vanishing positron density is used with the increased (relaxed) electron density.

The experimental positron lifetime for the (triply negative) Ga vacancy is 260 ps.[15] In order to reproduce this the ions neighboring the vacancy should relax inwards in all the schemes considered. The above comparison of the theoretical relative W parameters with the experimental ones also support this conclusion. The CONV and the two-component BN schemes give similar, relatively small (0.6–0.7 eV) trapping energies. They are in agreement with previous estimates,[6,7,11] which are typically smaller than those for metal vacancies.[29] The GGGC and the NOCORR schemes give substantially (by ~ 2 eV) larger positron trapping energies.

Next we consider the 2D-ACAR spectra calculated from the *valence* electron densities in the different schemes. The 2D-ACAR maps corresponding to the perfect bulk lattice and the ideal triply negative Ga vacancy calculated in the CONV scheme are shown in Fig. 7. The momentum density $\rho(\mathbf{p})$ of Eq. (18) is integrated along the $[1\bar{1}0]$ direction. The characteristic feature of the bulk distribution is the anisotropy with "shoulders" pointing to the [111] directions. The distribution for the vacancy is narrower due to the increase of the relative contribution of the annihilations with the low-momentum valence electrons. Also the shoulders have disappeared and only a slight anisotropy remains so that the contours reach further from the origin in the [110] direction that in the [100] direction. A comprehensive analysis of the momentum distributions for the bulk semiconductors as well as for their vacancies is due to Saito, Oshiyama, and Tanigawa.[32]

The cuts of 2D-ACAR spectra for the ideal Ga vacancy are shown in Figs. 7(c) and 7(d) along the [100] and [110] directions, respectively. All the curves are normalized to unity at zero momentum. The results calculated in the different schemes are compared with the experimental ones.[16] The narrowest and also the most isotropic distribution results in the GGGC scheme reflecting again the strong localization of the positron wave function at the vacancy. The CONV scheme gives a distribution that is, especially along the [110] direction, close to that of the GGGC scheme. The BN scheme gives results in the best agreement with the experiment. However, all the theoretical results for the ideal vacancy are too narrow and isotropic in comparison with the experimental 2D-ACAR distribution. The inward relaxation of the ions around the vacancy would again improve the situation by changing them towards the bulk result, which has a remarkable anisotropy [Fig. 7(a)].

B. Ion relaxations around a triply negative Ga vacancy in GaAs

In order to understand the effects of ion relaxation on the positron annihilation characteristics we have first performed calculations in which only the first neighbors of the vacancy are moved from their ideal lattice positions. In these calculations the ions are frozen to positions corresponding to a given amplitude of the breathing-mode relaxation conserving the T_d symmetry group of the ideal vacancy. This is consistent with the symmetry of the fully relaxed V_{Ga}^{3-} vacancy (see below). The total energies [Eq. (1)] of the electron-positron system calculated in the BN and GGGC schemes are given in Fig. 8(a) as a function of the amplitude of the relaxation. The CONV scheme results included in Fig. 8(a) refer to the model[11] in which the total energy is the sum of the pure electronic energy without the influence of the positron and the positron energy eigenvalue calculated within the CONV scheme. The results of the BN scheme and the CONV scheme nearly coincide. They show an energy minimum when the nearest-neighbor ions are moved inwards a distance, which corresponds to about 2% of the ideal lattice bond length. The similarity of these curves reflects the similarity of the positron energetics in these schemes. In the GGGC scheme the energy minimum is found to happen without any relaxation of the nearest-neighbor atoms. Especially in the CONV and BN schemes the total-energy curve is quite flat. The flatness would be even more pronounced if the ions beyond the nearest neighbors were allowed to relax and lower the total energy. The fact that the electronic total energy is a decreasing function of the inward relaxation whereas the positron energy eigenvalue rises when the open volume at the vacancy decreases is an important reason for the slow

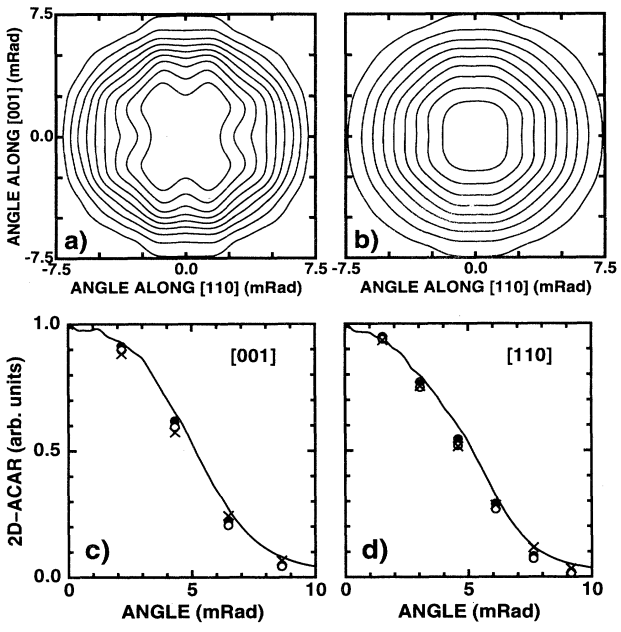

FIG. 7. Angular correlations of annihilation photons integrated along the $[1\bar{1}0]$ direction. The results for the perfect lattice (a), as well as for the ideal triply negative Ga vacancy in the conventional scheme (b) are shown. The contour spacing is one-tenth of the maximum value. The cuts along the [100] (c) and [110] (d) directions are given in the case of the Ga vacancy. The experimental results (Ref. 16) are given in (c) and (d) by solid lines, the results of the CONV (open circles), BN (solid circles), and GGGC (crosses) schemes are given at the discrete points for which the calculations are performed.

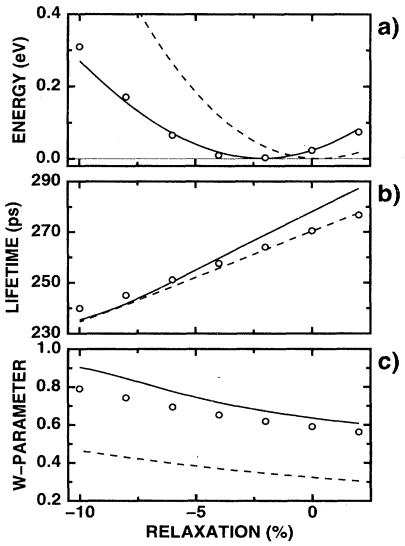

FIG. 8. Total energy (a), positron lifetime (b), and relative W parameter (c) for the triply negative Ga vacancy in GaAs trapping a positron. The results are given as functions of the breathing-mode relaxation of the ions neighboring the vacancy. The more distant ions are kept at the ideal lattice positions. The amplitude of the relaxation is given in percent of the bulk bond distance and negative (positive) values correspond to inward (outward) relaxation from the ideal lattice positions. The results of the BN (solid line), GGGC (dashed line), and CONV (open circles) schemes are shown.

variation of the total energy as a function of the ion relaxation. The flatness of the total energy means that the determination of the self-consistent ionic relaxations may be difficult, because the result may depend strongly on the approximations made.

The positron lifetime and the relative W parameter [Eq. (24)] are shown in Figs. 8(b) and 8(c), respectively. The results of the different schemes as a function of the relaxation of the nearest-neighbor ions of the vacancy are given. The positron lifetimes in the CONV and in the GGGC schemes are nearly identical due to the feedback mechanism explained above. The positron lifetime increases linearly when the ions relax outwards with the slope of about 3.5 ps/%. This is in accord with the previous theoretical estimations for the As vacancy in GaAs (Ref. 8) and with those for the vacancy in Si.[7] The slope in the BN scheme calculations is slightly larger, about 4.5 ps/%. The relative W parameter increases when the ions neighboring the vacancy relax inwards. The W parameters obtained in the CONV and BN schemes agree with the values, 0.7–0.8, of the coincidence Doppler experiment[31] if the ions neighboring the vacancy have relaxed slightly inwards. The W parameter obtained in the GGGC scheme is in clear disagreement with the experiment for all reasonable values of the relaxation.

Next we have allowed all the ions in the supercell to relax to the configuration corresponding to the minimum of the total energy. First the ionic relaxations and the electronic structure of the triply negative Ga vacancy are calculated without the trapped positron. Because all the localized electron states in the band gap are occupied, there is no strive for a symmetry-lowering Jahn-Teller relaxation and the relaxed vacancy conserves the T_d symmetry group. Thus the relaxation is of the pure breathing-mode type, and the atoms neighboring the vacancy relax inwards to the center of the vacancy by 10.7% of the ideal lattice bond length. This magnitude of the relaxation is clearly larger than the inward relaxation of about 4% found by Laasonen, Nieminen, and Puska[33] using a similar molecular-dynamics technique. However, the comparison of these results is not straightforward, for example, due to the different pseudopotentials used and the different lattice constants obtained. For comparison, the tight-binding calculation by Seong and Lewis[34] has given an inward relaxation of about 13%. The inward relaxation found in the present calculation is so strong that without the positron-induced relaxation the vacancy does not sustain a well-localized positron state neither according to the CONV scheme calculations nor according to any of the two-component schemes.

We then allow the ions around the vacancy to relax due to the introduction of the positron into the system. The resulting breathing-mode relaxations as well as the positron annihilation characteristics for the different two-component schemes are given in Table II. In all schemes the positron induces an outward ionic relaxation relative to the clean relaxed vacancy. According to the BN scheme the positron-induced relaxation is $\sim$4% of the bond length and the nearest-neighbor ions of the vacant site end up at positions that are a distance of 6.6% of the bond length inwards from the ideal lattice positions. This inward relaxation is stronger than that corresponding to the total-energy minimum in Fig. 8(a) because in the latter case ions beyond the nearest neighbors are not allowed to relax and thereby they hinder the relaxation of the nearest-neighbor atoms. In the GGGC scheme the effect of the localized positron is larger, the nearest-neighbor ions of the vacancy site end up at positions corresponding to an inward relaxation of 1.6% of the bond distance from the ideal lattice positions. The positron in this model is able to nearly heal the atomic positions around the vacancy to those of the ideal vacancy.

The inward relaxation found in the BN scheme is slightly too large in magnitude to reproduce the experimental positron lifetime. The positron wave function is not localized enough and the (scaled) positron lifetime obtained, 240 ps, is only slightly longer than the positron bulk lifetime of 231 ps. The W parameter has the value of 0.88, which is larger than those determined by the coincidence Doppler technique indicating also that the positron wave function is not localized enough. The posi-

TABLE II. Self-consistent solution for the electronic structure, positron state, and the ionic relaxations for the triply negative Ga vacancy in GaAs. The positron lifetime τ, core annihilation rate λ_c, valence annihilation rate λ_v, relative W parameter [Eq. (24)], the trapping energy E_t, and the amplitude d of breathing-mode relaxation relative to the bond length are given for the two-component BN, GGGC, and NOCORR schemes. BN4 refers to a calculation in which the nearest-neighbor ions of the vacancy are relaxed 4% of the bond length inwards from their ideal lattice positions and all the other ions are kept fixed. The lifetimes and annihilation rates are scaled so that the theoretical bulk lifetime coincides with the experimental one of 231 ps (Ref. 15). In the case of the GGGC and NOCORR schemes the lifetimes given in the parentheses are obtained using the two-component form of Eq. (22) depending on both the electron and positron densities. The positive (negative) sign of d means an outward (inward) breathing-mode relaxation.

Scheme	τ (ps)	λ_c (1/ns)	λ_v (1/ns)	W	E_t (eV)	d (%)
BN	240	0.468	3.684	0.88	0.09	−6.6
GGGC	268(306)	0.162	3.573	0.34	1.85	−1.6
NOCORR	272(308)	0.124	3.556	0.31	2.04	+3.0
BN4	260	0.354	3.498	0.72	0.27	−4.0

tron trapping energy is consistently relatively small, only 0.09 eV. On the contrary, the GGGC scheme results in too localized a positron state. Although the calculated positron lifetime of 268 ps is only slightly longer than the experimental one of 260 ps,[15] the calculated W parameter is by a factor of two too small, i.e., 0.34, indicating a much too small overlap of the positron with the core electrons. The positron trapping energy is also high, 1.9 eV. The NOCORR calculation gives again very similar results to the GGGC scheme. The positron-induced relaxation is slightly larger in the NOCORR scheme resulting in a somewhat longer positron lifetime, a smaller W parameter, and a larger positron binding energy. If the two-component enhancement, which depends also on the positron density, is used in the GGGC and NOCORR schemes, the positron lifetimes are longer than 300 ps.

The 3D-ACAR maps calculated in the BN and GGGC schemes for the self-consistently relaxed triply negative Ga vacancy are compared with the experimental one in Fig. 9. Compared with the experiment the GGGC scheme gives too narrow and isotropic a distribution, reflecting again the very localized nature of the positron wave function. The map corresponding to the BN scheme is more anisotropic, showing some bulklike features [compare with Fig. 7(a)], which is a signal of a somewhat too delocalized positron wave function.

The comparison of the calculated positron lifetimes, the relative W parameters, and the 2D-ACAR maps with the corresponding experimental ones indicates that the GGGC scheme results in too localized positron wave functions. In the first place, this is a result of the construction of the positron potential in the scheme; imposing a stronger inward relaxation of the ions neighboring the vacancy does not remedy this character as can be best seen in the behavior of the relative W parameter in Fig. 8(c). On the other hand, the BN scheme with the fully relaxed ion positions gives slightly too extended positron wave functions. This character, however, can be remedied by small changes in the ionic relaxation. For example, Figs. 8(b) and 8(c) indicate that the system, in which only the nearest-neighbor atoms of the Ga vacancy have relaxed inwards about 4% of the bond length, gives in the BN scheme a positron lifetime and relative W parameter, which are in good agreement with experimental values (the calculated values obtained are also given in Table II). This same system gives a 2D-ACAR map that according to Figs. 9(d) and 9(e) compared well with the measured one. The reason that the BN scheme does not give ion positions that reproduce accurately the experimental positron annihilation characteristics may lie in the approximations made in the calculations of the electron and positron structures. For example, the LDA for the electron exchange and correlation has been shown to overbind atoms so that the bond lengths in molecules and solids are too short.[35] This deficiency may also affect the relaxation of the ions around the defects.

The positron-induced relaxation has been estimated previously by Laasonen *et al.*[11] in the case of the neutral As vacancy in GaAs. These authors restricted the ionic relaxation to the pure breathing-type movement of the atoms neighboring the vacancy and used the CONV scheme in which the sum of the total electronic energy and the positron energy eigenvalue is minimized. In this model, the positron induces an outward relaxation of 4% of the bond length. Gilgien *et al.*[10] considered the positron state at the singly negative As vacancy in GaAs. Their calculation corresponds to the GGGC-scheme calculations; the most important differences are the use of a different pseudopotential for valence electrons and a more approximate treatment of the positron-ion core in-

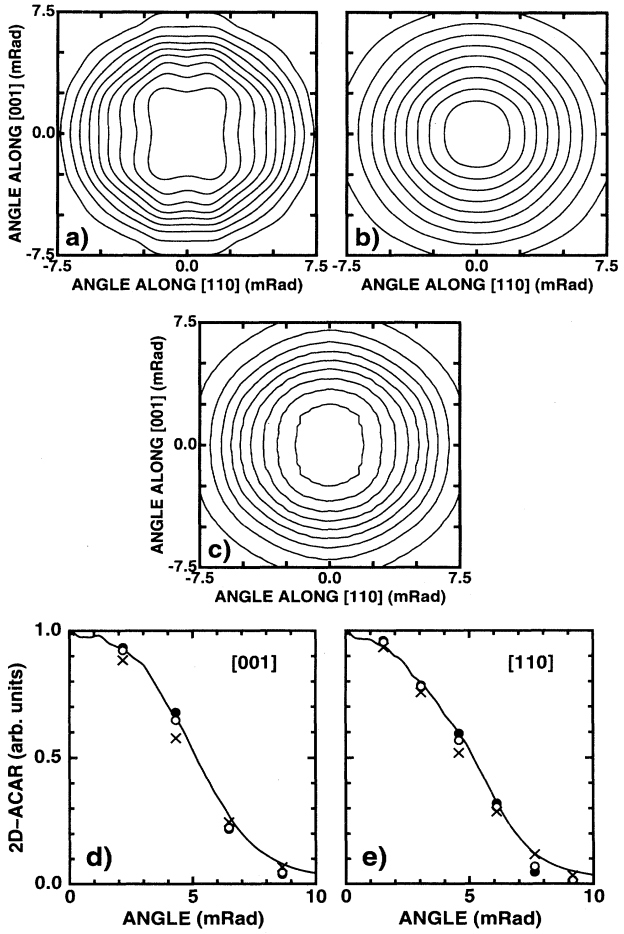

FIG. 9. Angular correlations of annihilation photons corresponding to the triply-negative Ga vacancy in GaAs. The momentum distributions are integrated along the [1$\bar{1}$0] direction. The results are based on the self-consistent solution for the electronic structure, positron state and the ionic positions at the vacancy within the two-component BN (a) and GGGC (b) schemes. The experimental map by Manuel *et al.* (Ref. 16) is also shown (c). The contour spacing is one tenth of the maximum value. The cuts along the [100] (d) and [110] (e) directions are shown. The experimental results (Ref. 16) are given in (d) and (e) by solid lines, the results of the BN (solid circles) and GGGC (crosses) schemes are given at the discrete points for which the calculations are performed. The open circles refer to BN-scheme calculations in which the nearest neighbor ions of the vacancy have relaxed inwards 4% of the bulk bond length.

teraction. Gilgien *et al.* found that the positron induces a strong outward relaxation of the ions neighboring the vacancy with low-symmetry ion configurations as a result. According to their calculations the positron lifetime increases strongly, about 50 ps. when the positron is trapped from the bulk state to the As vacancy. This is clearly more than the experimental increase of ~ 30 ps. A more accurate treatment of the positron-ion-core interaction may reduce the discrepancy. Gilgien *et al.* also calculated the 2D-ACAR map for the As vacancy and found, in agreement with our experience with the GGGC scheme for the Ga vacancy, a narrower and more isotropic distribution than the measured one.

IV. SUMMARY

We have developed a calculation scheme that solves self-consistently the electronic structure, positron state, and ion positions when a positron is trapped by a vacancy-type defect in a solid. The scheme is based on the two-component density-functional theory. The scheme is tested in the case of a triply negative Ga vacancy in GaAs with several descriptions for the electron-positron correlation. The calculated positron annihilation characteristics, i.e., the positron lifetime, the core annihilation parameter W, and the 2D-ACAR maps are compared with their experimental counterparts.

The scheme proposed by Boroński and Nieminen[9] for the electron-positron correlation gives descriptions for the positron potential and density that are similar to those obtained in the conventional scheme, in which the positron does not affect the average electron density. The positron state is in the BN scheme very sensitive to ion positions, and changes in the relaxation may change the positron annihilation characteristics remarkably. The scheme by Gilgien *et al.*[10] results in a more attractive positron potential at the defect and in a more localized positron wave function.

We find that at a clean triply negative Ga vacancy the nearest-neighbor ions have relaxed strongly inwards. The introduction of the positron at the vacancy induces a compensating outward relaxation, as this reduces the positron-ion repulsion. In the Boroński-Nieminen scheme the positron-induced relaxation is not very strong and the resulting positron lifetime is clearly shorter than the experimental value. However, small changes in the ion relaxations can bring the theoretical and experimental lifetimes into perfect agreement. This is true also for the other annihilation characteristics. In the Gilgien *et al.* scheme the positron-induced relaxation is stronger; it practically heals the vacancy to the ideal one. As a result the positron lifetime calculated is slightly longer than the experimental one. However, the W parameter is much too small and the 2D-ACAR maps too isotropic due to the strong positron localization.

For a given ionic configuration the conventional scheme predicts all positron annihilation characteristics considered in good agreement with the two-component Boroński-Nieminen scheme. This gives credence for the use of the conventional scheme in model calculations analyzing the experimental results by assuming reasonable ionic configurations for the defects. Due to a feedback effect the positron lifetimes from the conventional and Gilgien *et al.* schemes are nearly identical, although the W-parameters and 2D-ACAR maps differ remarkably. This means that especially the core annihilation W parameter determined for the defect is a sensitive quantity to describe the localization of the positron wave function in addition its high value in probing the chemical environments of defects in solids.

ACKNOWLEDGMENTS

The authors wish to thank R. Ambigapathy and A. A. Manuel for providing the experimental 2D-ACAR maps for the Ga vacancy in GaAs.

[1] *Positron Solid State Physics,* edited by W. Brandt and A. Dupasquier (North-Holland, Amsterdam, 1983); *Positron Spectroscopy of Solids,* Proceedings of the International School of Physics "Enrico Fermi," 1993, edited by A. Dupasquier and A. P. Mills, Jr. (North-Holland, Amsterdam, 1995).

[2] S. Berko, in *Momentum Distributions,* edited by R. N. Silver and P. E. School (Plenum, New York, 1989), p. 273.

[3] M. Alatalo, H. Kauppinen, K. Saarinen, M. J. Puska, J. Mäkinen, P. Hautojärvi, and R. M. Nieminen, Phys. Rev. B **51**, 4176 (1995).

[4] M. J. Puska and R. M. Nieminen, Rev. Mod. Phys. **66**, 841 (1994).

[5] *Deep Centers in Semiconductors,* edited by S. T. Pantelides (Gordon and Breach, New York, 1986); J. Dabrowski and M. Scheffler, Mater. Sci. Forum **83-87**, 735 (1992).

[6] M. J. Puska O. Jepsen, O. Gunnarsson, and R. M. Nieminen, Phys. Rev. B **34**, 2695 (1986).

[7] M. J. Puska and C. Corbel, Phys. Rev. B **38**, 9874 (1988).

[8] S. Mäkinen and M. J. Puska, Phys. Rev. B **40**, 12 523 (1989).

[9] E. Boroński and R. M. Nieminen, Phys. Rev. B **34**, 3820 (1986).

[10] L. Gilgien, G. Galli, C. Gygi, and R. Car, Phys. Rev. Lett. **72**, 3214 (1994).

[11] K. Laasonen, M. Alatalo, M. J. Puska, and R. M. Nieminen, J. Phys. Condens. Matter **3**, 7217 (1991).

[12] L. Lantto, Phys. Rev. B **36**, 5160 (1987).

[13] R. Car and M. Parrinello, Phys. Rev. Lett. **55**, 2471 (1985).

[14] M. C. Payne, M. P. Teter, D. C. Allan, T. A. Arias, and J. D. Joannopoulos, Rev. Mod. Phys. **64**, 1045 (1992).

[15] P. Hautojärvi, P. Moser, M. Stucky, C. Corbel, and F. Plazaola, Appl. Phys. Lett. **48**, 809 (1986); C. Corbel, F. Pierre, P. Hautojärvi, K. Saarinen, and P. Moser, Phys. Rev. B **41**, 10 632 (1990); C. Corbel, F. Pierre, K. Saarinen, P. Hautojärvi, and P. Moser, *ibid.* **45**, 3386 (1992).

[16] A. A. Manuel *et al.*, J. Phys. IV **5**, C1-73 (1995); see also R. Ambigapathy, A. A. Manuel, P. Hautojärvi, K. Saarinen, and C. Corbel, Phys. Rev. B **50**, 2188 (1994).

[17] R. Stumpf and M. Scheffler, Comput. Phys. Commun. **79**, 447 (1994).

[18]A. P. Seitsonen, M. J. Puska, and R. M. Nieminen, Phys. Rev. B **51**, 14 057 (1995).
[19]J. Perdew and A. Zunger, Phys. Rev. B **23**, 5048 (1981).
[20]J. Arponen and E. Pajanne, Ann. Phys. (N.Y.) **121**, 343 (1979); J. Phys. F **9**, 2359 (1979).
[21]E. Soininen, J. Mäkinen, D. Beyer, and P. Hautojärvi, Phys. Rev. B **46**, 13 104 (1992).
[22]K. O. Jensen, J. Phys. Condens. Matter **1**, 10 595 (1989).
[23]M. J. Puska, C. Corbel, and R. M. Nieminen, Phys. Rev. B **41**, 9980 (1990).
[24]D. R. Hamann, M. Schlüter, and C. Chiang, Phys. Rev. Lett. **43**, 1494 (1979). We use the pseudopotentials generated with the generalized scheme of the D. R. Hamann [Phys. Rev. B **40**, 2980 (1989)]. The nonlocality is treated using the technique proposed by L. Kleinmann and D. M. Bylander [Phys. Rev. Lett. **48**, 1425 (1982)].
[25]S. G. Louie, S. Froyen, and M. L. Cohen, Phys. Rev. B **26**, 1738 (1992).
[26]*Semiconductors. Physics of Group IV Elements and III-V Compounds,* edited by K.-H. Hellwege and O. Madelung, Landolt-Börnstein, New Series, Group III, Vol. 17, Pt. a (Springer-Verlag, Heidelberg, 1982).
[27]B. Barbiellini, M. J. Puska, T. Torsti, and R. M. Nieminen, Phys. Rev. B **51**, 7341 (1995).
[28]B. Barbiellini, M. J. Puska, T. Torsti, and R. M. Nieminen (unpublished).
[29]M. J. Puska and R. M. Nieminen, J. Phys. F **13**, 333 (1983).
[30]J. Mäkinen, T. Laine, K. Saarinen, P. Hautojärvi, C. Corbel, V. M. Airaksinen, and J. Nagle, Phys. Rev. B **52**, 4870 (1995).
[31]K. Saarinen *et al.* (unpublished).
[32]M. Saito, A. Oshiyama, and S. Tanigawa, Phys. Rev. B **44**, 10 601 (1991).
[33]K. Laasonen, R. M. Nieminen, and M. J. Puska, Phys. Rev. B **45**, 4122 (1992).
[34]H. Seong and L. J. Lewis, Phys. Rev. B **52**, 5675 (1995).
[35]For a recent review see R. O. Jones and O. Gunnarsson, Rev. Mod. Phys. **61**, 689 (1989).